Exploring anterior thalamus functional connectivity with cortical regions in prospective memory with ultra-high-field fMRI

Luke Flanagan[1], Bruno de Matos Mansur[1], Christoph Reichert[2], Anni Richter[2,3,4], Soroosh Golbabaei[5], Jasmin M. Kizilirmak[6,7,8], Catherine M. Sweeney-Reed[1,9*]

[1]Neurocybernetics and Rehabilitation, Dept. of Neurology, Otto von Guericke University, Magdeburg, Germany.
[2]Leibniz Institute for Neurobiology, Magdeburg, Germany
[3]German Center for Mental Health (DZPG), partner site Halle-Jena-Magdeburg, Germany
[4]Center for Intervention and Research on adaptive and maladaptive brain Circuits underlying mental health (C-I-R-C), Halle-Jena-Magdeburg, Germany
[5]Dept. of Psychiatry and Psychotherapy, Jena University Hospital, Jena, Germany
[6]Neurodidactics and NeuroLab, Institute of Psychology, University of Hildesheim, Germany
[7]German Centre for Higher Education and Science Research, Hannover, Germany
[8]German Center for Neurodegenerative Diseases, Göttingen, Germany
[9]Center for Behavioral Brain Sciences, Otto von Guericke University, Magdeburg, Germany

[*]Corresponding author:

Catherine M. Sweeney-Reed
Neurocybernetics and Rehabilitation, Dept. of Neurology, Otto von Guericke University, Magdeburg, Leipziger Str. 44, 39120 Magdeburg, Germany
catherine.sweeney-reed@med.ovgu.de

Abstract

Prospective memory (PM), or memory for future intentions, engages particular cortical regions. Lesion studies also implicate the thalamus, with PM deterioration following thalamic stroke. Neuroimaging, anatomical, and lesion studies suggest the anterior nuclei of the thalamus (ANT) in particular are involved in episodic memory, with electrophysiological studies suggesting an active role in selecting neural assemblies underlying particular memory traces. Here we hypothesized that the ANT are also engaged in realizing prospectively-encoded intentions, and that this engagement is detectable using ultra-high field strength functional MRI. Using a within-subject design, participants (N = 14; age 20-35 years) performed an n-back working memory task as the ongoing task with two cognitive loads, each with and without a PM component, during 7-Tesla functional MRI. Seed-to-voxel whole brain functional connectivity analyses were performed to establish whether including a PM component in an ongoing task results in greater connectivity between ANT and cortical regions known to be engaged in PM. Repeated measures ANOVAs were applied to behavioral and connectivity measures, with the factors *Task Type* (with PM or not) and *N-Back* (2-back or 3-back). Response accuracy was greater and reaction times faster without the PM component, and accuracy was higher in the 2- than 3-back condition. We observed a main effect of *Task Type* on connectivity with an ANT seed, with greater ANT–DLPFC (dorsolateral prefrontal cortex) and ANT–STG (superior temporal gyrus) connectivity when including a PM component. Post hoc testing based on a significant interaction showed greater ANT–DLPFC connectivity (p-FWE = .007) when PM was included with the low and ANT–STG connectivity (p-FWE = .019) with the high cognitive load ongoing task. These locations showed no main effect of *N-Back*. Connectivity based on a dorsomedial nucleus of the thalamus (DMNT) seed did not differ according to *Task Type* at these locations. Enhanced connectivity between the ANT and the DLPFC, a brain region with an established role in strategic monitoring for PM cues, arose with a low cognitive load ongoing task that enabled monitoring. This pattern was absent on directly increasing the cognitive load of the ongoing task without PM, suggesting specificity for PM. Greater ANT–STG connectivity on PM inclusion in the higher cognitive load ongoing task condition fits with reports of STG activation on PM through spontaneous retrieval. Differing connectivity based on a DMNT seed suggests ANT specificity. The findings fit with a coordinating role for the ANT in prospective remembering.

Keywords: prospective memory, anterior nuclei of the thalamus, 7T MRI, functional connectivity, strategic monitoring

Introduction

Prospective memory (PM), the ability to remember and fulfill future intentions[1–3], plays a pivotal role in essential tasks such as adhering to medication schedules and attending appointments. Notably, a decline in PM constitutes one of the most commonly reported memory concerns[4]. This cognitive function undergoes impairment with advancing age and is prevalent in conditions such as mild cognitive impairment and Parkinson's disease[5–8], emphasizing the urgency of unravelling its neural underpinnings for the development of effective diagnostic and therapeutic strategies. Neuroimaging and electrophysiological investigations consistently highlight the involvement of frontal and parietal cortical regions in PM[9–11]. Specifically, the dorsolateral prefrontal cortex (DLPFC) is engaged in both the maintenance and retrieval phases of PM[12–14]. Activation of a dorsal frontoparietal network is consistently observed during PM maintenance and deemed to reflect top-down attentional processes towards external PM cues and the content of prospectively-encoded intentions [9,10]. Furthermore, lesion studies underscore the critical role of the thalamus in PM, as evidenced by PM deterioration following thalamic stroke[15].

Neuroimaging and anatomical studies suggest the anterior nuclei of the thalamus (ANT) in particular are involved in episodic memory processing[16–19]. The ANT have been proposed to be part of an extended hippocampal system, based on their reciprocal anatomical connectivity with the hippocampus and their firing in the theta frequency range, the dominant hippocampal rhythm[16,20]. Lesion studies also indicate ANT involvement in episodic memory[15,21,22]. Evidence from intracranial recordings from the ANT of epilepsy patients suggests that the ANT play an active role in selection of neural assemblies underlying particular memory traces[18,19,23–25]. It is not known, however, whether such a role is specific to episodic memory events, or whether the ANT are engaged in coordinating the maintenance of prospectively encoded intentions.

Investigation of event-related PM classically involves the intention to perform a particular action, after a delay, on detection of a prospectively-encoded PM cue[5]. An important aspect is the performance of an ongoing task (OGT) that prevents continuous rehearsal of the PM task[5,26]. PM involves an integration of processes underlying episodic memory and also attentional processes. Based on engagement of different brain networks dependent on key aspects of a PM task, neurocognitive models have been proposed to explain how prospectively-encoded future intentions are realized. An influential model of how PM is performed is by either strategic monitoring of the environment for the PM cue, which involves a negative impact on OGT performance measures, by spontaneous retrieval of the PM task on PM cue detection, or by a combination[27]. The extent to which a particular approach is favored depends on the cognitive load involved in the OGT and PM cue features, such as the focality, saliency, and frequency[10,27–29].

Here we performed a seed-based functional connectivity (FC) analysis using a left ANT seed in a seed-to-voxel whole brain analysis to examine whether FC with cortical regions known to be engaged in PM is greater during performance of a task with a PM component than during a task condition comprising the OGT alone. We hypothesized that FC with the ANT would be detectable based on blood oxygen-dependent (BOLD) measurements acquired using 7-Tesla (7T) functional magnetic resonance imaging (fMRI) employing a block-design. Ultra-high magnetic field strength scanning results in a better signal-to-noise ratio (SNR) than using a low strength magnetic field, with a supralinear relationship between magnetic field strength and SNR[30]. Comparing using 7T with 3T field strength, subcortical structures in particular have been shown to be better discernable at the higher field strength[31]. Moreover, a 7T field strength has enabled detection of memory traces in the medial temporal lobe as well as differentiation between hippocampal subfields during associative learning[32,33]. The left ANT seed location was derived from a previous fMRI study investigating the role of the ANT and also the dorsomedial nucleus of the thalamus (DMNT) in episodic memory processing[17]. The hypothesis was based on a left ANT seed, because our paradigm, like that used by Pergola et al. (2013), can be performed using verbal-based strategies. Moreover, left lateralization has been previously associated with PM processing[14]. To assess the relevance of laterality, the seed location was mirrored to the right side for comparison. FC with a left DMNT seed was also examined, to evaluate the specificity of the engagement of the ANT. The classical n-back working memory (WM) task was used as the OGT[34–36], because the cognitive load can be readily adjusted, enabling assessment of whether differences in FC arising on adding the PM task result from increased cognitive load rather than PM processing.

Materials & Methods

Participants

Fourteen healthy participants aged 20-35 years were recruited among students at the Otto von Guericke University, Magdeburg. The mean age of the participants was 28.6 years (SD 3.3; 7 female). Participants all had normal or corrected to normal vision and no history of psychological or neurological disorders, regular medication, or recreational drug use. The study was approved by the Local Ethics Committee of the University Hospital, Magdeburg, in accordance with the Declaration of Helsinki. All participants provided informed, written consent prior to inclusion in the study and were informed of their right to cease participation at any time without providing reasons.

Behavioral paradigm

Visual stimuli were presented using Presentation software (Version 23.1 Build 09.20.22, Neurobehavioral Systems, Berkeley, CA, USA). The task comprised the n-back WM task as the OGT, with

a color-based PM task. Each trial comprised 500 ms presentation of a letter, and a jittered 1800-2100 ms response period. A sequence of letters was presented on a screen, and participants pressed one button when the current letter corresponded with the letter n letters previously and another button if not (Fig. 1A). The buttons were counterbalanced across participants. Each letter was presented in one of four colors (red/blue/green/yellow, specified in the RGB color space), assigned independently of the letter itself. The PM cue was a particular color, in response to which a third button was pressed with the thumb, instead of making an OGT (n-back) response. In other words, the PM cue indicated a brief task switch restricted to the respective trial, irrespective of which n-back response would have been correct.

The task comprised four variants: 2-back without a PM cue (2B); 2-back with a PM cue (2BPM); 3-back without a PM cue (3B); 3-back with a PM cue (3BPM). Each variant was performed four times, yielding a total of 16 runs per participant. The runs were carried out in a pseudorandom order, counterbalanced across participants, such that participants could perform low or high cognitive load variants first, as well as variants with or without PM first. Each run comprised 120 trials (lasting ~4 min). Based on previous studies, the PM conditions included 10% PM trials[28,37]. The OGT target rate of the current study was 15%.

Accuracy was quantified using d', a sensitivity measure based on the signal detection theory, given by the difference between z-scores of the proportions of hits and false alarms[38]. The accuracy and reaction times (RT) were analyzed using SPSS (IBM, New York). Mean d' and RTs were calculated for each participant. Two-way repeated measures ANOVAs were applied, with the within-subject factors *N-back* (2-Back, 3-Back) and *Task type* (OGT, OGT_PM), followed by post hoc tests. For effect size measures, we computed partial eta squared (η_p^2).

fMRI data acquisition

Structural and functional MRI data were recorded using a 7T MR scanner (Siemens MAGNETOM 7TPlus at the MRI Core Facility of the Otto von Guericke University Magdeburg). First, a T1-weighted magnetization-prepared rapid gradient echo (MPRAGE) image (TR = 2300 ms; TE = 2.73 ms; flip angle = 5°; 224 sagittal slices; FOV: 256 x 256 mm²; voxel size = 0.8 x 0.8 x 0.8 mm³) was acquired. This MPRAGE was used for the two-stage registration of the functional scans to the Montreal Neurological Institute (MNI) space. During the fMRI sessions, T2*-weighted echo-planar images (EPI; TR = 2000 ms; TE = 25 ms; flip angle = 75°; 81 axial slices; FOV: 212 x 212 mm²; voxel size = 1.5 x 1.5 x 1.5 mm³) were acquired, employing 3x multiband acceleration with GRAPPA parallel imaging (acceleration factor 2). During each of the sixteen 230 s runs, 115 volumes were acquired. All scans featured EPI distortion correction[39]. The first six scans during fMRI start-up were discarded.

Functional connectivity analysis

Analyses were performed using the Functional Connectivity Toolbox (CONN: Version 22[40,41] and SPM-12[42].

Pre-processing

Functional and anatomical data were pre-processed using a standard pre-processing pipeline, including realignment with correction of susceptibility distortion interactions, slice time correction, outlier detection, segmentation and normalization to the MNI space, using 4th order spline interpolation to re-slice functional data to yield 1.8 mm isotropic voxels, and smoothing[43]. Functional data were realigned using the SPM realign and unwarp procedure, where all scans were co-registered to a reference image (first scan of the first session) using a least squares approach and a 6-parameter rigid body transformation, and resampled using b-spline interpolation to correct for motion and magnetic susceptibility interactions[44,45]. Potential outlier scans were identified using ART (Artifact Detection Tools), as acquisitions with framewise displacement above 0.9 mm or global BOLD signal changes above 5 standard deviations[46–48], and a reference BOLD image was computed for each participant by averaging all scans excluding outliers. Functional and anatomical data were normalized into standard MNI space and segmented into grey matter, white matter, and cerebrospinal fluid (CSF) tissue classes using the SPM unified normalization and segmentation algorithm[49,50] and the IXI-549 tissue probability map template provided with CONN. Finally, the functional data were smoothed using spatial convolution with a Gaussian kernel of 3 mm full-width half maximum (FWHM).

The functional data were denoised using a standard denoising pipeline. The steps included the regression of potential confounding effects characterized by white matter time series (5 CompCor noise components), CSF time series (5 CompCor noise components), motion parameters and their first order derivatives (12 factors[43,51], outlier scans (below 14 factors[47], session and task effects and their first order derivatives (8 factors), and linear trends (2 factors) within each functional run. Regression was followed by bandpass frequency filtering of the BOLD time series[52] between 0.009 Hz and 0.08 Hz, as applied previously in fMRI studies using the n-back task[53,54]. CompCor[55,56] noise components within white matter and CSF were estimated by computing the average BOLD signal as well as the largest principal components orthogonal to the BOLD average, motion parameters, and outlier scans within each participant's eroded segmentation masks. From the number of noise terms included in this denoising strategy, the effective degrees of freedom of the BOLD signal after denoising were estimated to range from 143.7 to 438.9 (average 397.8) across all participants[48].

First-level analysis seed-based connectivity maps were estimated characterizing the spatial pattern of FC with a seed area. Three seed regions were analyzed. FC strength was represented by Fisher-

transformed bivariate correlation coefficients from a weighted general linear model (weighted-GLM[43], estimated separately for each seed area and target voxel, modelling the association between their BOLD signal time series. Individual time series were weighted by a boxcar signal characterizing each task or experimental condition convolved with an SPM canonical hemodynamic response function.

Group-level analyses were performed using a GLM framework, specifically employing a linear mixed-effects model to account for both fixed effects of the experimental conditions and random effects across participants. This approach allows for the analysis of voxel-level hypotheses by incorporating multivariate parametric statistics, which include variability across participants as random effects. Additionally, sample covariance estimation was used to account for variability across multiple outcome measures. Inferences were performed at the cluster level, based on parametric statistics from Gaussian Random Field theory[43,57]. Results were thresholded using a combination of a cluster-forming $p < 0.001$ voxel-level threshold, and a p-FWE < 0.05 cluster size threshold[58]. A left ANT seed, a mirror location in the right ANT, and a parvocellular division of left mediodorsal thalamic nucleus seed for the DMNT were used for seed-to-voxel FC analysis (Table 1). The MNI coordinates of the seeds were those reported in an fMRI study examining BOLD activity during a recognition and cued recall task using atlas-based regions of interest[17]. The locations chosen are described below.

Seed creation

The seeds, with 5-voxel radii (1 voxel = 1.8 mm), were created for each seed location in FSLeyes[59]. The location identified by Pergola *et al.* (2013; MNI: -3 -6 3) is located by the anterolateral border of the thalamus with the ventricle. As the volume of any seed at these coordinates, including a single voxel radius, created in FSLeyes using the MNI 2 mm brain, would overlap with the ventricle, the seed was placed five voxels medially, such that it was located entirely within the anterior thalamus. Seed 1 (MNI: -8 -6 3) is localized to the left anterior thalamus (Automated Anatomical Labelling atlas, version 3: AAL3[60], and the anterior–posterior location did not differ from that reported by Pergola et al. (2013) for the ANT. The seed location was also mirrored to the right side to examine potential laterality. While two other sets of ANT coordinates associated with memory retrieval were given, these locations were not localized by the AAL3 atlas to the ANT. Finally, a seed location in the DMNT from the same study (MNI: -6 -19.5 7.5), confirmed by AAL3 to be in left mediodorsal thalamus, was also used, to enable examination of whether any FC identified with Seed 1 was specific to the ANT.

Statistical analysis

A two-way repeated measures ANOVA was applied to the FC with each seed, with the factors *Task Type* (OGT, OGT_PM) and *N-Back* (2B, 3B), at voxel threshold < 0.001 and cluster size threshold $p < 0.05$. G*Power was used to calculate the power for the seed-based FC results post-hoc[61].

Results

Behavioral findings

Accuracy and RTs were normally distributed according to the Shapiro-Wilk test, with no outliers (defined as exceeding three times the interquartile range above the third or below the first quartile).

Main effects of *N-Back* (F[1,13] = 30.4, p < .001, η_p^2 = 0.70) and *Task Type* (F[1,13] = 6.1, p = .029, η_p^2 = 0.32) were observed. Post hoc testing showed that d' was greater during the OGT alone (mean d' = 1.69, 95% CI = [1.47 1.91]) than when the PM task was introduced (M = 1.56 [1.38 1.73]), and the d' was greater during 2B (M = 1.87 [1.65 2.10] than 3B (M = 1.37 [1.17 1.58]). There was no significant interaction.

A main effect of *Task Type* (F[1,13] = 21.0, p < .001, η_p^2 = 0.62) was observed for RTs, but no main effect of *N-Back* and no interaction (p > .05). Post hoc testing showed that the RTs were faster during the OGT alone (mean RT = 946 ms, 95% CI = [880 1013]) than when the PM task was introduced (mean RT = 1038 ms [974 1101]) (p < .001).

Functional connectivity

Seed 1: left ANT

Examining FC with Seed 1 in the ANT, clusters based on the applied significance thresholds (voxel threshold < .001; cluster size threshold p < .05) were identified with a minimum T-value of T(13) = 4.22, enabling detection of an effect with 0.98 power at an error probability of .05, and 0.58 at .001. Cluster locations where the cluster size p-FWE < .05 are given, together with cluster size, k.

A main effect of *Task Type* was observed in the left dorsolateral superior frontal gyrus according to the AAL3 atlas, in the DLPFC based on the cluster coordinates, and in the left superior temporal gyrus (STG) (Table 2). Based on the effect sizes, the FC with each cluster location was greater in the PM condition than in the OGT alone (Fig. 1B, C).

While a main effect of *N-Back* was also observed, the cluster locations differed from those showing a main effect of *Task Type*. Clusters were located in the right anterior prefrontal cortex and the left postcentral gyrus or somatosensory association cortex (Table 2).

An interaction between *Task Type* and *N-Back* was observed at the right inferior frontal gyrus, the right inferior occipital cortex, the left angular gyrus, and near to the right medial orbital superior frontal gyrus (Table 2).

Based on the interaction, post hoc comparisons were made. Contrasting the 2BPM with the 2B condition, FC was greater with left DLPFC, in a similar location to that identified as showing a main effect of *Task Type* (Fig. 2).

Contrasting the 3BPM with the 3B condition, greater FC was observed in the 3BPM than the 3B condition in the left and right STG, in a similar location to that identified as showing a main effect of *Task Type* (Fig. 3). Greater FC in the 3B than 3BPM condition was seen with the right medial superior frontal gyrus, the inferior frontal gyrus, and the right middle occipital gyrus.

Contrasting the 3B and 2B conditions, greater FC was seen in the 3B than the 2B condition with the right medial superior frontal gyrus and the right middle frontal gyrus (Fig. 4).

Finally, contrasting 3BPM with 2BPM, no cluster was significant following FWE correction.

Seed 2: right ANT

Applying an analogous ANOVA based on FC with the right ANT seed (Seed 2) also showed a main effect of *Task Type*, with clusters showing greater FC when a PM component was included than when the OGT was performed alone, at a location near to the superior/middle/inferior temporal gyri on the same side, and less FC at the pallidum, near the left ANT (Table 3). A main effect of *N-Back* was also observed, with clusters in the right cuneus, the left calcarine fissure, the right inferior temporal gyrus, and the right cerebellum. An interaction was seen, with a cluster in the left dorsolateral superior frontal gyrus (Table 3).

Based on the interaction, post hoc pairwise comparisons were performed (Table 3). Contrasting 2BPM with 2B, a cluster was seen in the contralateral (left) postcentral gyrus, with lower FC with Seed 2 in the PM condition. Contrasting the 3B and 2B conditions, greater FC was seen in the 3B condition in a region close to the left caudate and in the left medial superior frontal gyrus. Contrasting the 3BPM and 3B conditions, greater FC was seen in the 3BPM condition in a region close to the right pallidum. Finally, contrasting 3BPM with 2BPM, clusters were seen in the right calcarine fissure and the left inferior frontal gyrus.

Seed 3: left DMNT

An analogous ANOVA based on the left DMTN seed (Seed 3) revealed a main effect of *Task Type*, with clusters in the right inferior frontal gyrus, around the left pre- and post-central gyrus, and the left superior temporal gyrus, and a main effect of *N-Back*, with a cluster in the left middle occipital gyrus (Table 4). No significant interaction was seen.

Discussion

Supporting the hypothesis that the ANT play a role in coordinating PM processing, the left ANT showed greater FC with the left DLPFC and STG when a PM component was added to the OGT, a working memory task. FC between the left ANT and these regions was not observed when contrasting performance of the 2-back with the 3-back task, supporting the notion that the greater FC on introducing the PM task does not simply reflect greater cognitive load. This FC difference was not observed with the left DMNT, another thalamic nucleus engaged in declarative memory, pointing to a specific role for the ANT in PM processing.

Task performance strategy

The deterioration in performance of the OGT, reflected in lower accuracy and slower RTs in the OGT on addition of the PM component, suggests strategic monitoring for the PM cue. The lower OGT accuracy during the 3-back than the 2-back condition, with no change in RTs, is consistent with increased cognitive load during the 3-back condition[62]. The correct response rate to PM cues did not differ according to the OGT cognitive load, suggesting that strategic monitoring for a PM cue remained possible with the higher cognitive load, even if some spontaneous retrieval cannot be excluded.

The DLPFC has an established role in PM processing[13]. Activation of region BA 9 in particular has been associated with PM maintenance[9,63], and this area has also previously been associated with PM retrieval with a 2-back task as the OGT[64], as applied in the current study. Our finding of greater FC between the left ANT and BA 9 during PM maintenance is therefore consistent with engagement of the ANT in coordinating brain networks underpinning PM. Greater FC was also observed in the condition involving PM between the left ANT and the left STG as well as between the right ANT and right STG. The STG has been associated with top-down attentional processing and memory retrieval, and changes in FC between the STG and widespread cortical regions during stimulus maintenance in WM have led to the proposal of the STG as a hub region[10,65,66]. Notably the right STG was implicated in the latter WM study, which was suggested to be associated with the spatial nature of the particular WM task used (Park *et al.*, 2011). Modulation of STG activity has also been reported during processing of relationships between stimuli presented simultaneously[67]. This notion is interesting in the context of a PM paradigm, in which a single stimulus is presented but is simultaneously relevant to two different tasks, the OGT and the PM tasks. Taken together, these findings are consistent with strategic monitoring for a PM cue in the PM condition, with engagement of top-down attention, retrieval of the prospectively encoded intention, and dual-task processing. Indeed, PM tasks are a type of dual-task paradigm, particularly when the task requires task-switching and OGT inhibition[68].

Examining post hoc comparisons to FC with the left ANT seed, performed on the basis of the significant interaction, the contrast between FC in the 2BPM and 2B conditions corresponded with the main effect of *Task Type* observed in FC with DLPFC, while the contrast between FC in the 3BPM and 3B conditions showed greater correspondence with the main effect of *Task Type* seen in FC with the STG. These findings are consistent with a greater memory load in the 3-back conditions and more capacity for strategic monitoring when the overall cognitive load is lower, in the 2-back condition. While the behavioral findings indicate successful PM processing in the 3BPM condition, the FC results suggest that the PM task could be accomplished via a different mechanism, with a greater reliance on spontaneous retrieval. This interpretation fits with reports of more engagement of temporal regions in spontaneous retrieval[10,69].

Lateralization

Greater FC between the left ANT and both the DLPFC and STG is consistent with a role for the left ANT in the brain networks supporting PM. The finding is in keeping with previous reports of left lateralization of PM activity, which was suggested to reflect the lateralization of language processing to the left hemisphere[14]. It also fits with the memory-related activation in the left ANT in the study from which we derived the seed[17]. Using the seed location mirrored to the right ANT showed a remarkably similar FC difference, however, with an ipsilateral (right) temporal cluster showing greater FC with the right ANT seed in the PM condition than when the OGT was performed alone. We note that ANT–DLPFC FC was not observed with a right ANT seed, suggesting a laterality that could be attributed to the usage of letters in the n-back task and the lateralization of language in the left hemisphere in most right-handed individuals. We have previously observed modulation of electrophysiological activity in both the left and the right ANT during memory formation in a paradigm using visual scenes[23,25]. Given reports of laterality of ANT function and differences in FC here, engagement of left and right ANT in different functional networks is plausible, likely related to the modality of the paradigm, in which verbalization of the task is a potential strategy. Both ANT seeds showing greater FC with the STG does suggest engagement of the ANT on both sides in PM, however, albeit potentially in different ways.

Cognitive load

Given that adding a PM component has the potential to increase the cognitive load in the task, we also examined whether simply increasing the cognitive load of the OGT, by using a 3- rather than 2-back paradigm, would yield similar greater FC in contrast with the 2-back alone to that observed on adding the PM component. While greater frontal FC was observed, the frontal areas that were involved, BA 10/11 and BA 9/44, were more medial and anterior in location than the region of BA 9 (part of the DLPFC), where including a PM component was associated with greater FC than when the OGT was

performed alone. Of note also is that the FC with these regions was on the right side rather than the left, suggesting indirect FC as a part of a wider network. The finding is consistent with the suggestion that medial PFC is more active during an OGT requiring WM, with the lateral PFC underpinning delayed intentions[13]. BA 11 is also active in WM and the encoding of new information[70]. Encoding the next stimuli in a 3-back task could potentially require greater involvement of this region. BA 44, which is considered as part of the ventrolateral PFC, particularly on the right side, has been shown to be engaged in WM and motor response inhibition [71]. Given the lower number of targets than non-targets in the OGT, inhibition of a non-target response could be greater in the more challenging 3- than 2-back task.

Specificity of ANT

Lesion studies point to engagement of the thalamus in PM processing. To examine the specificity of a role for the ANT, we also examined seed-to-voxel whole brain connectivity with a seed located in another thalamic nucleus with an established role in episodic memory, the DMNT[17,72]. The DMNT projects to frontal cortex, and dissociations have been reported between the roles of the DMNT and ANT in memory processing, with the DMNT thought to play a predictive role in memory encoding and an executive role in memory retrieval[16,17,21,22,72]. While FC between the DMNT and left frontal areas differed according to whether a PM component was included in the task, the areas were not those usually reported to be engaged in PM and did not overlap with those showing FC with the ANT, suggesting that the ANT play a specific role in PM.

Limitations

Finally, we consider the sample size as a potential limitation. While larger participant groups are commonly included in fMRI studies at lower magnetic field strengths, comparatively lower participant numbers are reported to be required in 7T-fMRI studies[73,74]. In studies directly comparing analyses of data recorded at different field strengths, the ultra-high spatial specificity at 7T enables examination of fMRI at an individual participant level, so that 7T studies can be performed with smaller participant numbers than when scanning at lower field strengths[75,76]. Moreover, a recent study comparing memory consolidation using 7T and 3T fMRI with nine participants per group revealed expected changes in FC at 7T field strength, which were not detectable at 3T, even when correcting for SNR differences[77]. Differentiation between hippocampal subfields was possible in a group of fourteen participants during associative learning using 7T scanning[33], and memory traces were detected in the medial temporal lobe in eight participants at 7T[32]. The contrast between 7T and 3T field strengths that showed better discernment, particularly of subcortical structures, at 7T, was performed with ten participants[31]. Differences in subcortical–cortical FC involving another small, subcortical structure, the subthalamic

nucleus, and sensorimotor cortex were detected in a clinical study involving patient groups with twelve and 18 participants[78]. Future work should investigate whether these findings are replicable with different PM paradigms, to establish whether the ANT–cortical FC found here, when a PM component was added to the OGT, reflects essential mechanisms underpinning PM.

Conclusion

Our findings support our hypothesis that the ANT have a coordinatory role in PM processing. Increased FC was observed between the ANT and cortical areas previously reported to be engaged in PM. Previous evidence points to an active role for the ANT in episodic memory and for the thalamus in general in PM. Here we identified a specific co-activation of a frontal cortical area known to be associated with monitoring processes in prospective remembering and the ANT during PM processing, casting light on the mechanisms underpinning the retrieval of prospectively encoded future intentions. The finding was not replicated in a contrast in which the cognitive load of the working memory task was increased without PM, suggesting specificity for PM. Furthermore, the findings suggest that fMRI at an ultra-high field strength enables evaluation of FC with small, subcortical structures, including thalamic nuclei. A pivotal role for the ANT has potential implications both for patients with anterior thalamic lesions as well as for those receiving implantation of electrodes in the ANT for deep brain stimulation to treat pharmacoresistant epilepsy.

Data availability

The data that support the findings of this study are available upon reasonable request.

Acknowledgements

The authors would like to thank Dr. Claus Tempelmann for advice and assistance in design of the MRI data acquisition protocol.

Funding

This work was funded by the Forschung und Lehre Drittmittel (FULDM: Research and Teaching Funding) awarded to CMSR by the University Hospital Magdeburg based on receipt of funding from the Deutsche Forschungsgemeinschaft (German Research Council: SW214/2-1).

Competing ínterests

The authors have no conflicts of interest to declare.

References

1. Crowder R. The trouble with prospective memory: a provocation. In: Brandimonte M, Einstein G, McDaniel M, eds. *Prospective Memory: Theory and Applications,*. Lawrence Erlbaum Associates; 1996:143-147.

2. Kliegel M, Martin M, McDaniel MA, Einstein GO. Importance effects on performance in event-based prospective memory tasks. *Memory*. 2004;12(5):553-561. doi:10.1080/09658210344000099

3. Meacham JA, Singer J. Incentive effects in prospective remembering. *J Psychol*. 1977;97:191-197.

4. Kliegel M, Martin M. Prospective memory research: why is it relevant? *Int J Psychol*. 2003;38(4):193-194. doi:10.1080/00207590344000114

5. Einstein GO, McDaniel MA. Normal aging and prospective memory. *J Exp Psychol: Learning, Memory, and Cognition*. 1990;16(4):717-726. doi:10.1037/0278-7393.16.4.717

6. West R, Herndon RW, Covell E. Neural correlates of age-related declines in the formation and realization of delayed intentions. *Psychol Aging*. 2003;18(3):461-473. doi:10.1037/0882-7974.18.3.461

7. Costa A, Caltagirone C, Carlesimo GA. Prospective memory impairment in mild cognitive impairment: an analytical review. *Neuropsychol Rev*. 2011;21(4):390-404. doi:10.1007/s11065-011-9172-z

8. Costa A, Carlesimo GA, Caltagirone C. Prospective memory functioning: a new area of investigation in the clinical neuropsychology and rehabilitation of Parkinson's disease and mild cognitive impairment. Review of evidence. *Neurological Sciences*. 2012;33(5):965-972. doi:10.1007/s10072-012-0935-y

9. Cona G, Scarpazza C, Sartori G, Moscovitch M, Bisiacchi PS. Neural bases of prospective memory: a meta-analysis and the "Attention to Delayed Intention" (AtoDI) model. *Neurosci Biobehav Rev*. 2015;52:21-37. doi:10.1016/j.neubiorev.2015.02.007

10. McDaniel MA, Umanath S, Einstein GO, Waldum ER. Dual pathways to prospective remembering. *Front Hum Neurosci*. 2015;9:392. doi:10.3389/fnhum.2015.00392

11. Villafane Barraza V, Voegtle A, Mansur BDM, Reichert C, Nasuto SJ, Sweeney-Reed CM. Parietal cortical alpha/beta suppression during prospective memory retrieval. *Cerebral Cortex*. 2023;33(2):11235-11246. https://academic.oup.com/journals/pages/authors/authors_faqs/conflicts_of_interest.

12. Gilbert SJ, Gollwitzer PM, Cohen AL, Oettingen G, Burgess PW. Separable brain systems supporting cued versus self-initiated realization of delayed intentions. *J Exp Psychol Learn Mem Cogn*. 2009;35(4):905-915. doi:10.1037/a0015535

13. Burgess PW, Gonen-Yaacovi G, Volle E. Functional neuroimaging studies of prospective memory: what have we learnt so far? *Neuropsychologia*. 2011;49(8):2246-2257. doi:10.1016/j.neuropsychologia.2011.02.014

14. Cona G, Santacesaria P, Scarpazza C. Envisioning the future: an ALE meta-analysis on neural correlates of future thinking, prospective memory and delay discounting. *Neurosci Biobehav Rev*. 2023;153:105355. doi:10.1016/j.neubiorev.2023.105355

15. Carlesimo GA, Costa A, Serra L, Bozzali M, Fadda L, Caltagirone C. Prospective memory in thalamic amnesia. *Neuropsychologia*. 2011;49(8):2199-2208. doi:10.1016/j.neuropsychologia.2010.11.013

16. Aggleton JP, O'Mara SM, Vann SD, Wright NF, Tsanov M, Erichsen JT. Hippocampal-anterior thalamic pathways for memory: uncovering a network of direct and indirect actions. *Eur J Neurosci*. 2010;31(12):2292-2307. doi:10.1111/j.1460-9568.2010.07251.x

17. Pergola G, Ranft A, Mathias K, Suchan B. The role of the thalamic nuclei in recognition memory accompanied by recall during encoding and retrieval: an fMRI study. *Neuroimage*. 2013;74:195-208. doi:10.1016/j.neuroimage.2013.02.017

18. Sweeney-Reed CM, Buentjen L, Voges J, et al. The role of the anterior nuclei of the thalamus in human memory processing. *Neurosci Biobehav Rev*. 2021;126:146-158. doi:10.1016/j.neubiorev.2021.02.046

19. Sweeney-Reed CM, Knight RT. Memory and the human anterior thalamus. In: Usrey WM, Sherman SM, eds. *The Cerebral Cortex and Thalamus*. First. Oxford University Press; 2023.

20. Vertes RP, Albo Z, Viana di Prisco G. Theta-rhythmically firing neurons in the anterior thalamus: implications for mnemonic functions of Papez's circuit. *Neuroscience*. 2001;104(3):619-625. doi:10.1016/S0306-4522(01)00131-2

21. Harding A, Halliday G, Caine D, Kril J. Degeneration of anterior thalamic nuclei differentiates alcoholics with amnesia. *Brain*. 2000;123(1):141-154. doi:10.1093/brain/123.1.141

22. van der Werf YD, Jolles J, Witter MP, Uylings HBM. Contributions of thalamic nuclei to declarative memory functioning. *Cortex*. 2003;39:1047-1062. doi:10.1016/S0010-9452(08)70877-3

23. Sweeney-Reed CM, Zaehle T, Voges J, et al. Corticothalamic phase synchrony and cross-frequency coupling predict human memory formation. *Elife*. 2014;3:e05352. doi:10.7554/eLife.05352

24. Sweeney-Reed CM, Zaehle T, Voges J, et al. Thalamic theta phase alignment predicts human memory formation and anterior thalamic cross-frequency coupling. *Elife*. 2015;e07578:1-9. doi:10.7554/eLife.075781of9

25. Sweeney-Reed CM, Zaehle T, Voges J, et al. Anterior thalamic high frequency band activity is coupled with theta oscillations at rest. *Front Hum Neurosci*. 2017;11:358. doi:10.3389/fnhum.2017.00358

26. Guynn MJ. A two-process model of strategic monitoring in event-based prospective memory: activation/retrieval mode and checking. *Int J Psychol*. 2003;38(4):245-256. doi:10.1080/00207590344000178

27. Einstein GO, Thomas R, Mayfield S, et al. Multiple processes in prospective memory retrieval: Factors determining monitoring versus spontaneous retrieval. *J Exp Psychol: General*. 2005;134(3):327-342. doi:10.1037/0096-3445.134.3.327

28. Wilson J, Cutmore TRH, Wang Y, Chan RCK, Shum DHK. Effects of cue frequency and repetition on prospective memory: an ERP investigation. *Int J Psychophysiol*. 2013;90(2):250-257. doi:10.1016/j.ijpsycho.2013.08.003

29. Cona G, Chiossi F, Di Tomasso S, et al. Theta and alpha oscillations as signatures of internal and external attention to delayed intentions: A magnetoencephalography (MEG) study. *Neuroimage*. 2020;205. doi:10.1016/j.neuroimage.2019.116295

30. Pohmann R, Speck O, Scheffler K. Signal-to-noise ratio and MR tissue parameters in human brain imaging at 3, 7, and 9.4 tesla using current receive coil arrays. *Magn Reson Med*. 2016;75(2):801-809. doi:10.1002/mrm.25677

31. Colizoli O, de Gee JW, van der Zwaag W, Donner TH. Functional magnetic resonance imaging responses during perceptual decision-making at 3 and 7 T in human cortex, striatum, and brainstem. *Hum Brain Mapp*. 2022;43(4):1265-1279. doi:10.1002/hbm.25719

32. Vanasse TJ, Boly M, Allen EJ, et al. Multiple traces and altered signal-to-noise in systems consolidation: evidence from the 7T fMRI Natural Scenes Dataset. *PNAS*. 2022;119(44):e2123426119. doi:10.1073/pnas

33. Suthana NA, Donix M, Wozny DR, et al. High-resolution 7T fMRI of human hippocampal subfields during associative learning. *J Cogn Neurosci*. 2015;27(6):1194-1206. doi:10.1162/jocn_a_00772

34. Scharinger C, Soutschek A, Schubert T, Gerjets P. Comparison of the working memory load in n-back and working memory span tasks by means of EEG frequency band power and P300 amplitude. *Front Hum Neurosci*. 2017;11:1-19. doi:10.3389/fnhum.2017.00006

35. Röhner F, Breitling C, Rufener KS, et al. Modulation of working memory using transcranial electrical stimulation: a direct comparison between TACS and TDCS. *Front Neurosci*. 2018;23(12):761. doi:10.3389/fnins.2018.00761

36. Voegtle A, Reichert C, Hinrichs H, Sweeney-Reed CM. Repetitive anodal TDCS to the frontal cortex increases the P300 during working memory Processing. *Brain Sci*. 2022;12(11):1545. doi:10.3390/brainsci12111545

37. West R. The cognitive neuroscience of prospective memory. In: Kliegel M, McDaniel M, Einstein G, eds. *Prospective Memory: Cognitive, Neuroscience, Developmental, and Applied Perspectives*. Taylor & Francis Group/Lawrence Erlbaum Associates; 2008:261-282.

38. Green D, Swets J. *Signal Detection Theory and Psychophysics*. Wiley.; 1966.

39. In MH, Speck O. Highly accelerated PSF-mapping for EPI distortion correction with improved fidelity. *Magnetic Resonance Materials in Physics, Biology and Medicine*. 2012;25(3):183-192. doi:10.1007/s10334-011-0275-6

40. Whitfield-Gabrieli S, Nieto-Castanon A. Conn: a functional connectivity toolbox for correlated and anticorrelated brain networks. *Brain Connect*. 2012;2(3):125-141. doi:10.1089/brain.2012.0073

41. Nieto-Castanon A, Whitfield-Gabrieli S. *CONN Functional Connectivity Toolbox: RRID SCR_009550, Release 22*. Hilbert Press; 2022. doi:10.56441/hilbertpress.2246.5840

42. Friston KJ. *Statistical Parametric Mapping. The Analysis of Functional Brain Images*. Academic Press; 2011.

43. Nieto-Castanon A. *Handbook of Functional Connectivity Magnetic Resonance Imaging Methods in CONN*. Hilbert Press; 2020. doi:10.56441/hilbertpress.2207.6598

44. Friston KJ, Ashburner J, Frith CD, Poline JB, Heather JD, Frackowiak RSJ. Spatial registration and normalization of images. *Hum Brain Mapp*. 1995;2:165-189.

45. Andersson JLR, Hutton C, Ashburner J, Turner R, Friston KJ. Modeling geometric deformations in EPI time series. *Neuroimage*. 2001;13(5):903-919. doi:10.1006/nimg.2001.0746

46. Whitfield-Gabrieli S, Nieto-Castanon A, Ghosh S. Artifact detection tools (ART). Release version 7:11. Cambridge, MA: Artifact Detection Tools.

47. Power JD, Mitra A, Laumann TO, Snyder AZ, Schlaggar BL, Petersen SE. Methods to detect, characterize, and remove motion artifact in resting state fMRI. *Neuroimage*. 2014;84:320-341. doi:10.1016/j.neuroimage.2013.08.048

48. Nieto-Castanon A. Preparing fMRI Data for statistical analysis. *ArXiv*. Published online 2022:1-25. doi:10.48550/arXiv.2210.13564

49. Ashburner J, Friston KJ. Unified segmentation. *Neuroimage*. 2005;26(3):839-851. doi:10.1016/j.neuroimage.2005.02.018

50. Ashburner J. A fast diffeomorphic image registration algorithm. *Neuroimage*. 2007;38(1):95-113. doi:10.1016/j.neuroimage.2007.07.007

51. Friston KJ, Williams S, Howard R, Frackowiak RSJ, Turner R. Movement-related effects in fMRI time-series. *Magn Reson Med*. 1996;35:346-355. doi:10.1002/mrm.1910350312

52. Hallquist MN, Hwang K, Luna B. The nuisance of nuisance regression: spectral misspecification in a common approach to resting-state fMRI preprocessing reintroduces noise and obscures functional connectivity. *Neuroimage*. 2013;82:208-225. doi:10.1016/j.neuroimage.2013.05.116

53. Philip NS, Sweet LH, Tyrka AR, et al. Early life stress is associated with greater default network deactivation during working memory in healthy controls: a preliminary report. *Brain Imaging Behav*. 2013;7(2):204-212. doi:10.1007/s11682-012-9216-x

54. Yang H, Zhang J, Jin Z, Bashivan P, Li L. Using modular connectome-based predictive modeling to reveal brain-behavior relationships of individual differences in working memory. *Brain Struct Funct*. 2023;228(6):1479-1492. doi:10.1007/s00429-023-02666-3

55. Behzadi Y, Restom K, Liau J, Liu TT. A component based noise correction method (CompCor) for BOLD and perfusion based fMRI. *Neuroimage*. 2007;37(1):90-101. doi:10.1016/j.neuroimage.2007.04.042

56. Chai XJ, Castañán AN, Öngür D, Whitfield-Gabrieli S. Anticorrelations in resting state networks without global signal regression. *Neuroimage*. 2012;59(2):1420-1428. doi:10.1016/j.neuroimage.2011.08.048

57. Worsley KJ, Marrett S, Neelin P, et al. A unified statistical approach for determining significant signals in images of cerebral activation. *Hum Brain Mapp*. Published online 1996:458-473. doi:10.1002/(SICI)1097-0193

58. Chumbley J, Worsley K, Flandin G, Friston KJ. Topological FDR for neuroimaging. *Neuroimage*. 2010;49(4):3057-3064. doi:10.1016/j.neuroimage.2009.10.090

59. McCarthy P. Source code: FSLeyes. Zenodo.

60. Rolls ET, Huang CC, Lin CP, Feng J, Joliot M. Automated anatomical labelling atlas 3. *Neuroimage*. 2020;206. doi:10.1016/j.neuroimage.2019.116189

61. Faul F, Erdfelder E, Lang AG, Buchner A. G*Power 3: a flexible statistical power analysis program for the social, behavioral, and biomedical sciences. *Behav Res Meth*. 2007;39(2):175-191. doi:10.3758/BF03193146

62. Pelegrina S, Lechuga MT, Garcï¿½a-Madruga JA, et al. Normative data on the n-back task for children and young adolescents. *Front Psychol*. 2015;6(OCT):1-11. doi:10.3389/fpsyg.2015.01544

63. Okuda J, Fujii T, Yamadori A, et al. Participation of the prefrontal cortices in prospective memory: evidence from a PET study in humans. *Neurosci Lett*. 1998;253:127-130. doi:10.1016/s0304-3940(98)00628-4

64. Gilbert SJ, Armbruster DJN, Panagiotidi M. Similarity between brain activity at encoding and retrieval predicts successful realization of delayed intentions. *J Cogn Neurosc*. 2012;24(1):93-105. doi:10.1162/jocn_a_00094

65. Hopfinger JB, Buonocore MH, Mangun GR. The neural mechanisms of top-down attentional control. *Nat Neurosci*. 2000;3(3):284-291. http://neurosci.nature.com

66. Park H, Kang E, Kang H, et al. Cross-frequency power correlations reveal the right superior temporal gyrus as a hub region during working memory maintenance. *Brain Connect*. 2011;1(6):460-472. doi:10.1089/brain.2011.0046

67. Proskovec AL, Wiesman AI, Heinrichs-Graham E, Wilson TW. Beta oscillatory dynamics in the prefrontal and superior temporal cortices predict spatial working memory performance. *Sci Rep*. 2018;8(1). doi:10.1038/s41598-018-26863-x

68. Bisiacchi PS, Schiff S, Ciccola A, Kliegel M. The role of dual-task and task-switch in prospective memory: behavioural data and neural correlates. *Neuropsychologia*. 2009;47(5):1362-1373. doi:10.1016/j.neuropsychologia.2009.01.034

69. Beck SM, Ruge H, Walser M, Goschke T. The functional neuroanatomy of spontaneous retrieval and strategic monitoring of delayed intentions. *Neuropsychologia*. 2014;52(1):37-50. doi:10.1016/j.neuropsychologia.2013.10.020

70. Frey S, Petrides M. Orbitofrontal cortex: a key prefrontal region for encoding information. *PNAS*. 2000;97(15):8723-8727. www.pnas.orgcgidoi10.1073pnas.140543497

71. Neef NE, Bütfering C, Anwander A, Friederici AD, Paulus W, Sommer M. Left posterior-dorsal area 44 couples with parietal areas to promote speech fluency, while right area 44 activity promotes the stopping of motor responses. *Neuroimage*. 2016;142:628-644. doi:10.1016/j.neuroimage.2016.08.030

72. Sweeney-Reed CM, Zaehle T, Voges J, et al. Pre-stimulus thalamic theta power predicts human memory formation. *Neuroimage*. 2016;138:100-108. doi:10.1016/j.neuroimage.2016.05.042

73. Hua J, Blair NIS, Paez A, et al. Altered functional connectivity between sub-regions in the thalamus and cortex in schizophrenia patients measured by resting state BOLD fMRI at 7T. *Schizophr Res*. 2019;206:370-377. doi:10.1016/j.schres.2018.10.016

74. Sbaihat H, Rajkumar R, Ramkiran S, et al. Test–retest stability of spontaneous brain activity and functional connectivity in the core resting-state networks assessed with ultrahigh field 7-Tesla resting-state functional magnetic resonance imaging. *Hum Brain Mapp*. 2022;43(6):2026-2040. doi:10.1002/hbm.25771

75. Viessmann O, Polimeni JR. High-resolution fMRI at 7 Tesla: challenges, promises and recent developments for individual-focused fMRI studies. *Curr Opin Behav Sci*. 2021;40:96-104. doi:10.1016/j.cobeha.2021.01.011

76. Willems T, Henke K. Imaging human engrams using 7 Tesla magnetic resonance imaging. *Hippocampus*. 2021;31(12):1257-1270. doi:10.1002/hipo.23391

77. Kreitz S, Mennecke A, Konerth L, et al. 3T vs. 7T fMRI: capturing early human memory consolidation after motor task utilizing the observed higher functional specificity of 7T. *Front Neurosci*. 2023;17. doi:10.3389/fnins.2023.1215400

78. Evangelisti S, Boessenkool S, Patrick Pflanz C, et al. Subthalamic nucleus shows opposite functional connectivity pattern in Huntington's and Parkinson's disease. *Brain Commun*. 2023;5(6). doi:10.1093/braincomms/fcad282

Tables

Table 1. MNI coordinates for seed locations (adapted from coordinates from Pergola *et al.*, 2013).

Seed	Location	Side	x	y	z
1	anterior nuclei of the thalamus	L	-8	-6	3
2	anterior nuclei of the thalamus	R	8	-6	3
3	dorsomedial nucleus of the thalamus	L	-6	-19.5	7.5

Seed 2 was mirrored to the right side from the coordinates for the left side (Seed 1) by inversing the x-coordinates. ANT: anterior nuclei of the thalamus; MDpc = parvocellular division of mediodorsal thalamic nuclei; L: left; R: right

Table 2. Functional connectivity with the left ANT (Seed 1) according to *Task Type* and *N-Back*.

MNI-coordinates	Cluster location	Brodmann's area	Cluster size	T(13)	p-FWE
Main effect of *Task type*					
-22 38 42	left dorsolateral superior frontal gyrus (DLPFC)	BA 9	39	7.07	.0070
-54 -28 10	left superior temporal gyrus	BA 22	33	7.65	.019
Main effect of *N-Back*					
06 44 00	right anterior prefrontal cortex	BA 10/11	63	8.01	.0018
-16 -44 70	left postcentral gyrus: primary somatosensory cortex	BA 2	42	-7.58	.0047
Interaction between *Task type* and *N-Back*					
52 24 22	right inferior frontal gyrus	BA 45	33	-6.87	.021
24 -98 -08	right inferior occipital gyrus	BA 18	32	-5.74	.025
-50 -70 26	left angular gyrus	BA 39	30	-7.5	.035
04 66 -18	near right medial orbital superior frontal gyrus	BA 48	29	-6.20	.042
Post hoc test of main effect of *Task type*: 2BPM vs. 2B					
-16 42 44	left dorsolateral superior frontal gyrus (DLPFC)	BA 9	59	7.85	.00028

Post hoc test of main effect of *Task type*: 3BPM vs. 3B: 3BPM > 3B					
-48 -30 06	left superior temporal gyrus	BA 48	143	10.26	<.000001
52 -18 04	right superior temporal gyrus	BA 48	75	10.55	.000037
Post hoc test of main effect of *Task type*: 3BPM vs. 3B: 3B > 3BPM					
4 40 50	right medial superior frontal gyrus	BA 8	45	-7.91	.0030
48 24 20	right inferior frontal gyrus	BA 48	44	-10.10	.0035
44 -78 22	right middle occipital gyrus	BA 39	31	-7.13	.031
Post hoc test of main effect of *Task type*: 3B vs. 2B					
04 46 00	right medial superior frontal gyrus	BA 10/11	50	6.91	.0012
50 10 50	right middle frontal gyrus	BA 9/44	30	6.02	.035

BA: Brodmann's area

Table 3. Functional connectivity with the right ANT (Seed 2) according to *Task type* and *N-Back*.

MNI-coordinates	**Cluster location**	**Brodmann's area**	**Cluster size**	**T(13)**	**p-FWE**
Main effect of *Task Type*: OGT_PM > OGT alone					
48 -26 -10	near right superior/middle/inferior temporal gyri	BA 48	37	9.16	.0096
Main effect of *Task Type*: OGT alone > OGT_PM					
-12 6 -4	left pallidum (near left ANT)	-	83	7.36	.00001
Main effect of *N-Back*					
10 -88 14	right cuneus	BA 18	86	-12.1	.000006
-8 -90 -4	left calcarine fissure	BA 17	64	-8.11	.00012
60 -38 -20	right inferior temporal gyrus	BA 20	32	8.63	.021
26 -58 -46	right cerebellum	BA 48	30	8.64	.031
Interaction between *Task Type* and *N-Back*					
-12 56 28	left dorsolateral superior frontal gyrus	BA 9	36	6.33	.0094

Post hoc test of main effect of *Task Type*: 2BPM vs. 2B: 2BPM > 2B					
-32 -28 40	near left postcentral gyrus	-	30	-9.38	.032
Post hoc test of main effect of *Task Type*: 3B vs. 2B					
-04 12 12	near left caudate	-	32	8.76	.022
-6 52 8	left medial superior frontal gyrus	BA 10	28	6.78	.047
Post hoc test of main effect of *Task Type*: 3BPM vs. 3B					
22 -6 02	right pallidum	BA 48	43	8.34	.0031
Post hoc test of main effect of *Task Type*: 3BPM vs. 2BPM					
12 -90 4	right calcarine fissure	BA 17	32	7.56	.018
-48 26 24	left inferior frontal gyrus	BA 48	29	-8.2	.032

BA: Brodmann's area

Table 4. Functional connectivity with the left DMTN (Seed 3) according to *Task type* and *N-Back*.

MNI-coordinates	**Cluster location**	**Brodmann's area**	**Cluster size**	**T(13)**	**p-FWE**
Main effect of *Task Type*: OGT_PM > OGT alone					
58 34 08	right inferior frontal gyrus	BA 45	45	7.98	.0027
-54 -12 46	near left pre-/ post-central gyrus	BA 4	41	9.62	.0052
-44 0 -8	left superior temporal gyrus	BA 48	29	8.98	.042
Main effect of *N-Back*					
-50 -78 6	left middle occipital gyrus	BA 19	56	-8.32	.0004

BA: Brodmann's area

Figures

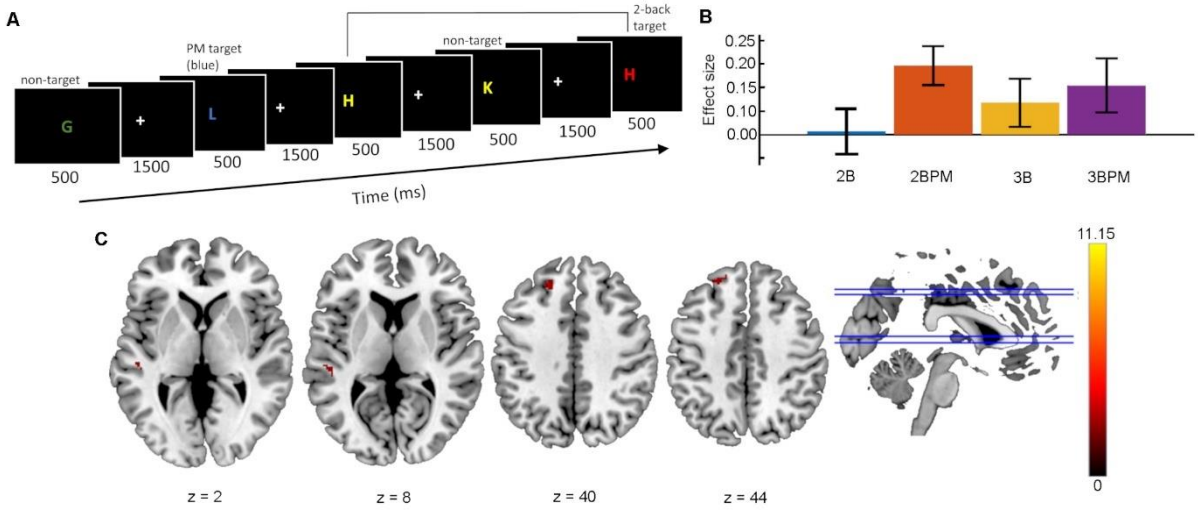

Figure 1. Functional connectivity with the left anterior nuclei of the thalamus during prospective remembering. **A**. Behavioural paradigm. Illustration of the 2-back task, with the colour blue as the PM cue. **B**. Effect sizes in the four task conditions at the cluster locations where a main effect of *Task type* was observed. 2B: 2-back only; 2BPM: 2-back with PM component; 3B: 3-back only; 3BPM: 3-back with PM component. Cluster MNI coordinates are given below. **C**. Functional connectivity based on a seed in the anterior nuclei of the thalamus (Seed 1), with clusters showing the main effect of *Task Type*. Greater connectivity in the conditions including a PM component can be seen in the left dorsolateral superior frontal gyrus (p-FWE = .007) and the left super temporal gyrus (p-FWE = .019).

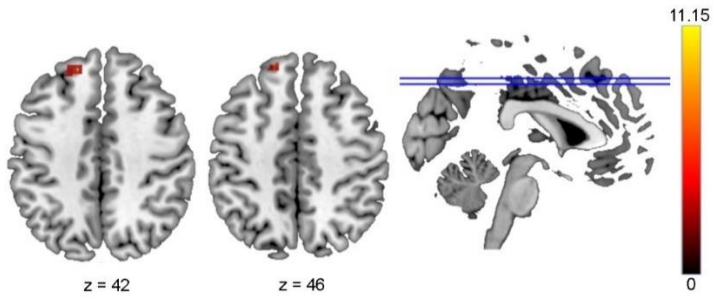

Figure 2. Functional connectivity (FC) difference between 2BPM and 2B conditions based on a seed in the anterior nuclei of the thalamus (Seed 1). Greater FC was observed in the 2BPM than the 2B condition with the left dorsolateral superior frontal gyrus (p-FWE = .00028).

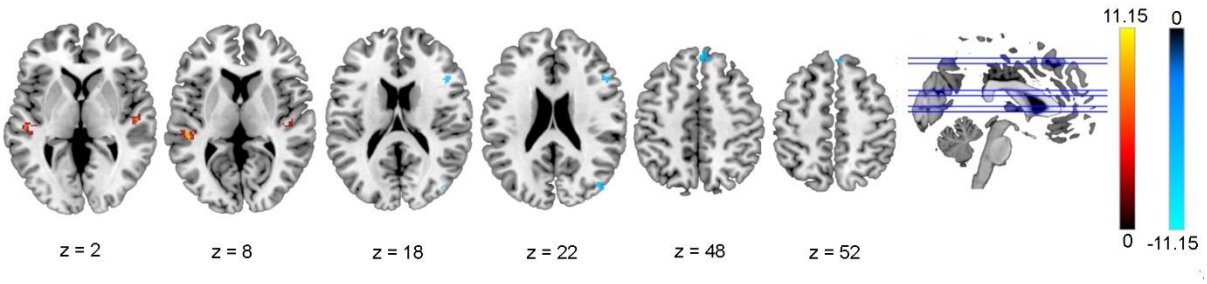

Figure 3. Functional connectivity (FC) difference between 3BPM and 3B conditions based on a seed in the anterior nuclei of the thalamus (Seed 1). Greater FC was observed in the 3BPM than the 3B condition in the in the left (p-FWE < .000001) and right superior temporal gyri (p-FWE = .000037). Greater FC in the 3B than 3BPM condition was seen with the right medial superior frontal gyrus (p-FWE = .0030), the inferior frontal gyrus (p-FWE = .0035), and the right middle occipital gyrus (p-FWE = .031).

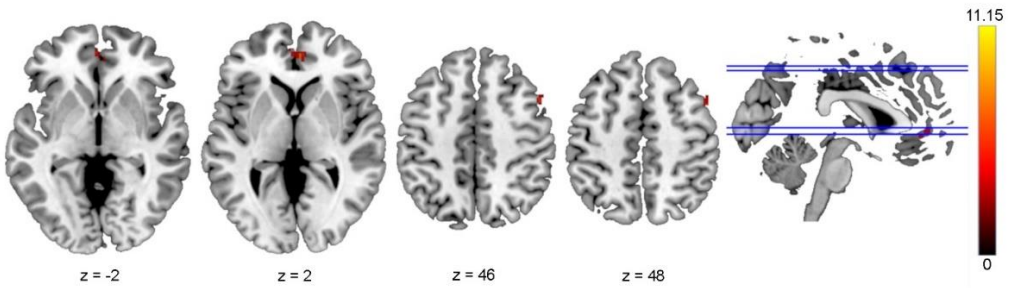

Figure 4. Functional connectivity (FC) difference between 3B and 2B conditions. Greater FC was observed in the right medial superior frontal gyrus (p-FWE = .0012) and in the right middle frontal gyrus (p-FWE = .035).